Available online at www.sciencedirect.com
ScienceDirect
International Journal of Heat and Mass Transfer 50 (2007) 539–551
International Journal of HEAT and MASS TRANSFER
www.elsevier.com/locate/ijhmt

Reduced-order modeling of turbulent forced convection with parametric conditions

Jeffrey Rambo [a], Yogendra Joshi [b,*]

[a] Shell Global Solutions Houston, TX 77210, United States
[b] G.W. Woodruff School of Mechanical Engineering, Georgia Institute of Technology, Atlanta, GA 30332, United States

Received 14 December 2005; received in revised form 21 July 2006
Available online 23 October 2006

Abstract

Accurate reduced-order models of turbulent flows have been traditionally constructed with the proper orthogonal decomposition (POD), however the method has been limited to prototypical flows over a narrow parameter range. An orthogonal complement subspace method is developed here to treat inhomogeneous boundary conditions while implicitly coupling the velocity and temperature fields of turbulent convection. A new flux matching procedure is formulated as a state space residual series expansion to efficiently model parameter dependent convection, greatly extending the utility of the reduced-order modeling framework. An illustrative test case of turbulent channel flow over heated blocks shows flow and thermal models with 95% accuracy over the domain can be produced, while simultaneously reducing the number of degrees of freedom by a factor of 10^3. Error bounds are formulated and provide *a posteriori* error estimates for the reduced-order model.

Keywords: Reduced-order modeling; Turbulent forced convection

1. Introduction

Design and analysis of complex engineering systems involving turbulent convection often require careful numerical simulations using computational fluid dynamics and heat transfer (CFD/HT) or detailed experimental data, such as that obtained by full field techniques such as tomographic interferometry and particle image velocimetry to accurately describe the fluid flow and heat transfer processes of the system [1]. Both methods of system characterization are time intensive, particularly so for carrying out parametric studies. In early stages of design, it may be desirable to trade this effort for an experimentally validated reduced model that captures the dominant physics, but is computationally efficient. Such models may be used in conjunction with optimization routines to quickly perform parameter sensitivity studies. A low-dimensional model of this type can also be integrated with multi-scale computations to efficiently bridge a range of length scales without requiring a single simulation to model all length scales simultaneously.

Methods of reduced-order modeling can generally be divided into state space and distributed parameter system approaches. State space methods reduce a system to an input/output map and many tools are available to analyze interconnected state space components, see [2] for an application-based overview. Distributed parameter systems aim to approximate the physics over the entire domain, as opposed to returning a vector of desired outputs. This approach is desirable in modeling convective flows, as the model is not limited to returning a prescribed quantity, such as a set of velocity, temperature or heat flux information, rather the complete velocity and temperature fields are available for further analysis of the transport processes involved. The fundamental principle of distributed parameter modeling is to find a suitable set of modes to project

* Corresponding author.
E-mail addresses: jeff.rambo@shell.com (J. Rambo), yogendra.joshi@me.gatech.edu (Y. Joshi).

0017-9310/$ - see front matter © 2006 Published by Elsevier Ltd.
doi:10.1016/j.ijheatmasstransfer.2006.07.029

Nomenclature

a, b	modal weight coefficient
c	mode scaling constant
d	subspace distance
e	error
k_{eff}	effective thermal conductivity
m	number of observations
n	number of system DOF
p	number of retained modes
r	residual
s	number of control surfaces
$\vec{u}$	velocity field
E	spectral energy
F	flux function
G	goal
J	error functional
P	orthogonal projection matrix
Q	power dissipation
T	temperature field
v_{eff}	effective viscosity
$\vec{\varphi}$	velocity mode
ψ	temperature mode

Greek symbols

λ	eigenvalue
ρ	fluid density

Subscripts

0	source function
h	heat
i	in-plane
m	mass
o	out-of-plane

Superscripts

$+$	matrix pseudo-inverse
*	approximate solution
’	orthogonal complement, dual space
obs	observational data
$\sim$	projected solution

the governing equations onto, reducing the solution procedure to finding the appropriate weight coefficients that combine the modes into the desired approximate solution.

A *parametric system* is defined here as a system containing a source term or boundary condition that can be varied over a specified range in order to produce different system responses. For a convective flow, such parameters include a geometrical length, mass flow rate, boundary heat flux or temperature, or volumetric heat generation, to produce different flow patterns, and/or transport characteristics. This can be quantified with one or more relevant dimensionless groups, such as Reynolds or Strouhal number, non-dimensional heat generation rates, or a set of aspect ratios to define geometry. Changes in thermophysical property variations are excluded from this definition because they may arise naturally even in the absence of the parametric variabilities defined here. In summary, the parametric nature may result from a prescribed boundary condition, for example inlet velocity or wall heat flux, interior condition, such as volumetric heat generation, or geometric parameter such as an aspect ratio.

2. POD analysis of convective systems with parametric variations

The proper orthogonal decomposition (POD) is a stochastic tool used to assemble the model-specific optimal linear subspace from an ensemble of system observations. Owing to the stochastic nature of the subspace calculations, the POD is ideally suited for nonlinear phenomena and has been used extensively in low-dimensional modeling of turbulent flows, see [3] for a more complete description and review. A major shortcoming of the existing POD methodology to date is its inefficient treatment of a range of model parameters. Previous reduced-order flow and heat transfer modeling studies have investigated the dynamics of a prototypical system under a single Reynolds or Rayleigh number or limited range of variation. Laminar flows were investigated by Deane et al. [4] and ad hoc mode scaling showed mixed results (±15% in period predictions) for approximating flows from 52 observations over a small range of Reynolds numbers. For laminar flows with various inlet profiles, both Park and Kim [5] and Ravindran [5–7] suggest homogenizing the POD modes by subtracting a reference field that satisfies the governing equations. Park and Kim [5] constructed a low-dimensional controller for flow over a backward facing step based on 1000 observations of two inlet velocity profiles. Ravindran homogenized 100 observations for developing a flow controller using blowing at $Re = 200$ [6,7]. In the investigation of transitional behavior, Ma and Karniadakis used 40 modes to study the limit cycle of three-dimensional flow around a cylinder at a critical $Re = 188$ [8] and at $Re = 610$ [1]. No special boundary treatment was required for either flow because periodic boundary conditions were employed.

In low order modeling of heat transfer, Park and Cho partitioned the linear governing equation into homogeneous and inhomogeneous components to account for boundary conditions in order to model conduction [9] and temperature and species transport for a fixed velocity

field [10], using 200 and 400 observations respectively. Sirovich [11–13] analyzed the dynamics of natural convection by working with homogeneous deviations from the mean flow, allowing the mean to take the inhomogeneous boundary conditions and typically using around 200 observations. Park and Li [14] modeled natural convection with 30 sinusoidal boundary heat flux profiles for a total of 3000 observations.

Recent developments in low-dimensional flow modeling have been made by Sirisup and Karniadakis [15] who have proposed using a penalty function Galerkin method to treat time varying boundary conditions. Geometrical scaling has also been investigated by Taylor and Glauser [16] who constructed a low-dimensional model of a variable angle diffuser at the expense of 30,720 observations. Uttakar et al. [17] used POD for reduced turbulent simulations of flows with moving boundaries; however they do not describe any reduced-order model development, only the accuracy and data compression associated with POD representation of the observations. Galletti et al. [18] modeled laminar flow over a confined square block by interpolating the modal weight coefficients at different Reynolds number to correct the pressure drop across the duct from 160 observations. To summarize the work to date in developing POD-based models of flows over a range of varying Reynolds and Rayleigh numbers, inhomogeneous boundary conditions are either treated through expensive homogenization procedures or through a very large, and often impractical, number of system observations.

A key concern in the existing POD methodology is determining the minimum number of observations required to construct a POD subspace that faithfully represents the physics of the system. In dynamic systems simulation, each simulation time step is available to be included in the ensemble. Experimentally-based POD models of turbulent flows also benefit from large data ensembles, as many repeated measurements are required to generate stochastically significant turbulence statistics. For parametric reduced-order modeling of stationary turbulent flows, the focus of the present study, each observation is from an independent system snapshot. For maximum computational efficiency, special consideration is given to the minimum number of observations and associated error. To the best of the author's knowledge, the only published attempt of using POD-based modeling for stationary analysis of thermo-fluid systems was by Ly and Tran [19]; however their solution method was based on interpolating splines between weight coefficients to match a desired parameter value. This method would require higher order multi-dimensional interpolation to model a complex system with multiple parameters and also does not guarantee that the desired parameter level will be achieved.

The modeling framework is developed through a reformulation of the proper orthogonal decomposition (POD). Orthogonal complement subspaces are introduced to parameterize the POD modes as a function of the varying boundary conditions, based on the ideas set forth by Christensen et al. [20] and Jorgensen et al. [21]. In working with Reynolds-averaged Navier–Stokes (RANS) simulations, the standard method of Galerkin projection of the governing equations on the POD subspace is impossible without additional effort to specify the effective viscosity. Further, Rempfer [22] demonstrates that the Galerkin projection can produce unstable dynamical systems and ultimately lead to unphysical results. A new method for computing the modal weight coefficients is to use a state space residual series expansion, thereby greatly improving the solution efficiency and eliminating the computational cost and instabilities associated with the Galerkin projection. This method has been demonstrated to be very successful in constructing low-dimensional models of parametric boundary driven turbulent flows [23] and to the best of the author's knowledge is the only RANS-based POD modeling methodology [24]. This methodology is extended in the current paper to incorporate the energy equation to create low-dimensional models of turbulent convection. The results indicate parameter dependent turbulent forced convection flows spanning a range of Reynolds numbers and heat fluxes can be reduced into accurate low-dimensional models, to be employed in design and optimization studies.

3. Model parameters

The methodology is illustrated for a RANS simulation of two-dimensional duct flow of air over two aluminum heated blocks in tandem (see Fig. 1). The geometry is identical to the experimental measurements of Yoo et al. [25], whose data were used to validate the turbulence modeling in the CFD/HT code. The steady, incompressible, constant properties RANS continuity, momentum and energy equations without external forcing or buoyancy effects are:

$$\nabla \cdot \vec{u} = 0, \tag{1a}$$

$$\vec{u} \cdot \nabla \vec{u} - \nabla \cdot (\nu_{\text{eff}} \nabla \vec{u}) + \frac{1}{\rho} \nabla P = 0, \tag{1b}$$

$$\rho c_{\text{p}} \vec{u} \cdot \nabla T - \nabla \cdot (k_{\text{eff}} \nabla T) = 0, \tag{1c}$$

where $\nu_{\text{eff}} = \nu + C_\mu \frac{k^2}{\varepsilon}$ and $k_{\text{eff}} = k + \frac{c_{\text{p}} \nu_{\text{t}}}{\rho Pr_{\text{t}}}$ with $Pr_{\text{t}} = 0.85$ and can be computed through any RANS-based turbulence model. The standard k–ε model with non-equilibrium wall functions [26] was used to model the effect of turbulence on the mean flow and the inlet velocity, turbulent kinetic energy and turbulent dissipation rate boundary profiles were calculated assuming a fully developed flow. The fully converged CFD/HT model consisted of 10,000 grid cells and solving for two velocity components, pressure, k and ε at

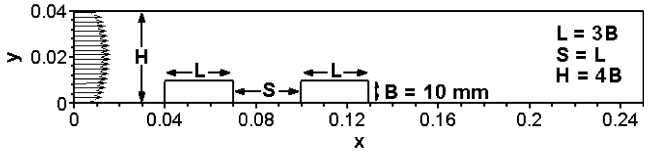

Fig. 1. Model geometry from Yoo et al. [25].

each grid cell resulted in approximately 50,000 degrees of freedom (DOF) to model the flow. The solution was demonstrated to be independent of grid size and convergence criteria, and each solution required approximately 500 iterations to converge.

The flow parameter range of the model was chosen to be $13{,}690 \leqslant Re \leqslant 41{,}070$, for $Re = \rho B\bar{u}/\mu$ which corresponds to an average velocity of $5.0 \leqslant \bar{u} \leqslant 15.0$ m/s in air, and the block power was assumed to range from 25 to 200 W. The inlet temperature was fixed at 288 K and all fluid properties were evaluated at this temperature. All results will be reported as the temperature rise above this nominal value. Table 1 summarizes the set of observations used to construct the reduced-order model subspace. The heat input to each block was applied as a uniform heat flux on the bottom surface ($y = 0$). The local Nusselt number ($Nu = hB/k$), using a running coordinate over the surface of blocks, is plotted against the experimental data of Yoo et al. [25] in Fig. 2. The numerical simulation agrees fairly well with the experimental data with some error in magnitude over the surface of the first block. Chen et al. [27] have experimentally investigated a similar geometry for similar Reynolds numbers and have suggested the standard low Reynolds number turbulence model of Jones and Launder [28] provides accurate local heat transfer coefficient predictions. The code is based on wall functions and the pressure-gradient sensitive wall functions employed provide the most accurate results without significant code modifications. It should also be noted that the mesh employed here is of similar size to that of Chen et al., even though the wall functions are used in this investigation while the Jones–Launder low Reynolds number model relies on a damping function to model the near wall effects. Detailed computations of flow and heat transfer characteristics of periodic blocks in a rectangular channel is presented in [29].

The basic motivation of low-dimensional modeling is to create a more computationally efficient way of reproducing the physics described by a high fidelity numerical simulation or detailed experimental dataset. It is important to note that both numerical and experimental observations will depart somewhat from the true system behavior. The purpose of this investigation is to present a reduced-order modeling framework for turbulent forced convection, not to model a particular system. Thus, the numerical data will be treated as the 'exact' system response in the description of the methodology below, and some discussion of various errors and their contribution to total error will be subsequently provided.

Table 1
Observation database

k	Re	$\bar{u}$	Q_1 (W)	Q_2 (W)
1	13,692	5	25	200
2	16,430	6	50	175
3	19,168	7	50	100
4	21,907	8	100	150
5	24,645	9	125	175
6	27,383	10	100	100
7	30,122	11	200	175
8	32,860	12	100	75
9	35,599	13	200	125
10	38,337	14	200	50
11	41,075	15	200	25

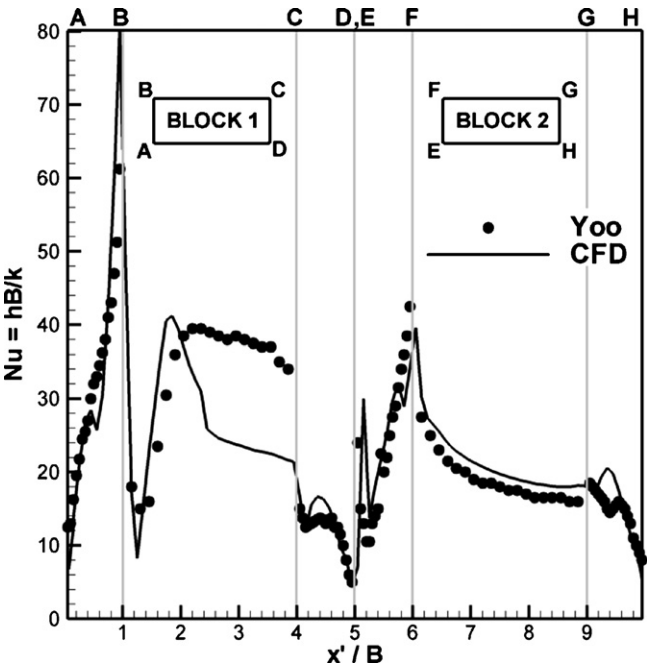

Fig. 2. Comparison of numerical solution at $Re = 13{,}690$, with the experiments of Yoo et al. [25].

4. POD reduced-order modeling methodology

This section contains a brief overview of the POD, with [3] providing an extensive description of the method and its previous use in the analysis of turbulent flows. The POD uses principal component analysis to decompose a large DOF system into a series of fundamental modes and an approximation to the governing equations is sought using the expansion theorem:

$$u(x,t) = \sum_{i=1}^{m} a_i(t)\varphi_i(x). \tag{2}$$

Solution methods based on (2) require the specification of a family of functions forming the modal basis $\Phi = \{\varphi_1, \varphi_2, \ldots, \varphi_m\}$ that span the domain Ω. The basis functions usually satisfy homogeneous boundary conditions individually and inhomogeneous boundary conditions are treated by adding a source function:

$$\vec{u}(x,t) = \vec{u}_0(x,t) + \sum_{i=1}^{m} a_i(t)\vec{\varphi}_i(x). \tag{3}$$

Note in the most general case the source function, $\vec{u}_0$, may account for time dependent boundary conditions. In the context of convection, the solution and modal basis will

be considered vector-valued functions. In traditional POD analysis of turbulent flows, the source function in (3) often assumes the form of the ensemble mean, $\vec{u}_0 = \langle \vec{u} \rangle$, which renders the POD modes akin to the Reynolds stresses.

The POD is a stochastic tool that computes the optimal linear basis for the modal decomposition in (3). Given an ensemble of system observations, $\{\vec{u}_k \in H | k = 1, 2, \ldots, m\}$, $\vec{\Phi}$ can be computed by minimizing the projection error onto the ensemble, $\min\{\langle \|\vec{u}_k - P_k \vec{u}_k\| \rangle\}$ where P_k is the orthogonal projector, $\|\cdot\|$ is the induced norm on the Hilbert space H and $\langle \cdot \rangle$ denotes the ensemble average. For discrete data m observations of the system containing n DOF are assembled into the observation matrix $\vec{U} = \{\vec{u}_1, \vec{u}_2, \ldots, \vec{u}_m\} \in R^{n \times m}$. The empirical basis functions (referred to as 'POD modes') are then computed as a linear combination of the linearly independent observations, known as the method of snapshots, see [30], viz,

$$\vec{\varphi}(x) = \sum_{i=1}^{m} b_i \vec{u}_i(x). \tag{4}$$

The weight coefficients in (4) are the eigenvectors of $(1/m)\vec{U}^{\mathrm{T}}\vec{U} \in R^{m \times m}$, allowing the number of observations and not the number of system DOF to dictate the size of the basis function computation. Using the method of snapshots to assemble the basis functions as admixtures of the system observations implies that $\vec{\Phi}$ intrinsically contains any linearly invariant properties of $\vec{u}_k$ from the fact that $\vec{\Phi}$ has been computed only through linear operations on $\vec{U}$. Thus, the POD modes individually satisfy the incompressibility condition, $\nabla \cdot \vec{\varphi}_k = 0 \quad \forall k$ and homogeneous boundary conditions, $\vec{\varphi}(\partial\Omega) = 0$ where $\vec{u}(\partial\Omega) = 0$.

From an implementation standpoint, the POD mode may be computed by assembling the observation matrix $\vec{U} = \{\vec{u}_1, \vec{u}_2, \ldots, \vec{u}_m\} \in R^{n \times m}$ and then decomposing $\vec{U}$ using the singular value decomposition (SVD). Given a matrix $A \in R^{n \times m}$, the SVD produces the decomposition $A = U\Sigma V^{\mathrm{T}}$ where $U \in R^{n \times n}$ is a matrix whose columns form the left singular vectors of A, $V \in R^{m \times m}$ is a matrix whose columns form right singular vectors of A and Σ is a pseudo-diagonal matrix of the singular values. It can be shown that $A^{\mathrm{T}}A = V\Sigma^2 V^{\mathrm{T}}$ with eigenvalues equal to $\lambda_k = \sqrt{\Sigma_{kk}}$. The method of snapshots can be implemented as $B = \mathrm{SVD}(\vec{U}^{\mathrm{T}}\vec{U})$ with $B \in R^{m \times m}$ and then assembling $\vec{\Phi} = \vec{U}B$. The energy captured by each POD mode is then computed as $E_k = \frac{\lambda_k}{\sum_{k=1}^{m} \lambda_k}$ and the total energy resolved using the first p modes $E_{1 \to p} = \frac{\sum_{k=1}^{p} \lambda_k}{\sum_{k=1}^{m} \lambda_k}$.

5. Low-dimensional turbulent flow modeling

The modal weight coefficients in the expansion (3) for a new solution $\vec{u}^*$ can generally be computed as $a_i = (\vec{u}^*, \vec{\varphi}_i)$. However, $\vec{u}^*$ is unknown, and the only feature that is known about the new solution are the boundary conditions. The standard procedure in the POD methodology would be to substitute in the model expansion of (3) into (1b) and project the governing Eq. (1b) onto the POD subspace through the Galerkin procedure, viz,

$$\int_{\Omega} \vec{\varphi}_i \cdot (\vec{u} \cdot \nabla \vec{u} - \nabla \cdot (\nu_{\mathrm{eff}} \nabla \vec{u}) + \frac{1}{\rho} \nabla P) = 0. \tag{5}$$

Eq. (5) could be solved along with a set of constraints in order to enforce the boundary conditions [22], although no guarantee can be made that the boundary conditions will be satisfied. The POD modal basis of (3) contains velocity field information only. Examination of the k–ε model shows the turbulence transport equations are functions of velocity gradients only, thus the RANS momentum equation can be viewed as a model for a laminar flow with a strain-rate dependent viscosity. A practical implication of reduced-order models of RANS-based simulations is that the number of retained modes is on the order of previous laminar flow investigations ($<10^2$), as opposed to reduced-order models derived from direct numerical simulation data which retain ($>10^3$) modes, because the fine scale details of the turbulence transport are modeled in the eddy viscosity.

The k and ε transport equations could be evaluated by substituting the velocity modes into the governing equations, but the boundary conditions would need to be specified. Moreover, this would require operating point-wise on the velocity field, violating the fundamental idea of distributed parameter model reduction which is to find a suitable set of modes to project the governing equations onto and then evaluate the weight coefficients. All the previously discussed low-dimensional flow investigations have used the Navier–Stokes equations as the governing equations, either through analyzing laminar flows or utilizing higher order spectral methods on fine enough meshes such that all relevant turbulence transport length scales are resolved. RANS-based POD presents the unique problem of not being able to evaluate the governing equations without specifying the effective viscosity. It will be shown that given a series of systems observations an accurate low-dimensional model can still be realized, making this method well suited for inverse problems.

6. RANS-based POD

Since the POD modes are themselves solutions to the governing Eqs. ((1a)–(1c)), new solutions can be generated by using inhomogeneous modes to satisfy the boundary conditions and letting the structure of the POD modes resolve the flow field over the remainder of the domain. Since the POD basis is the optimal linear subspace for a given dataset, the approximate analysis is treated as a linearized boundary value problem. This assumes the modal contribution can be uniquely determined by satisfying the boundary conditions.

Ensuring that only the boundary conditions are satisfied and ignoring the residual over the rest of the domain is a familiar concept. Using information from only a small subset of the entire domain to estimate the velocity field is

commonly used in flow control because it is impractical to distribute sensors through the entire flow field. One such example used of linear stochastic estimation to correlate pressure measurements at the wall and POD modal coefficients to develop a low-dimensional flow controller [16].

In the analysis of complex flows, the exact velocity profile on the boundary is often unknown. However, the design objective is often based on integral conditions, such as the appropriate mass flux through a portion of the boundary, prompting the introduction of the mass flux function:

$$F_m(\vec{u}) = \int_{\Gamma_m} \rho \vec{u} \cdot \hat{n} \mathrm{d}x, \quad \Gamma_m \subseteq \Omega. \tag{6}$$

This function generally returns a vector because Γ_m may be a finite set of discontinuous surfaces. A new approximate solution can be expressed as the vector of goals $G_m \in R^s$ corresponding to the desired mass flux through the set of control surfaces $\Gamma = \{\Gamma_1, \Gamma_2, \ldots, \Gamma_s\}$ that define the desired flow field $\vec{u}^*$ such that $G = F(\vec{u}^*)$. The solution procedure is then to find the set of weight coefficients that minimizes the error on the set of control surfaces Γ_m:

$$\min \left\{ \left\| G_m - \sum_{i=1}^{p} a_i F_m(\vec{\varphi}_i) \right\| \right\}, \quad p \leqslant m. \tag{7}$$

The solution procedure is carried out as a series expansion with the ordered POD modes forming the expansion sequence and terms are successively added to the series until the boundary conditions are satisfied. Algorithmically, this can be expressed as:

$$\Delta G_{m,i} = G_{m,i-1} - F_m(\vec{u}_{i-1}), \tag{8a}$$

$$a_i = F_m^+(\vec{\varphi}_i) \Delta G_{m,i}, \tag{8b}$$

$$\vec{u}_i = \vec{u}_0 + \sum_{j=1}^{i} a_j \vec{\varphi}_j, \tag{8c}$$

where $F^+() \equiv (F^{\mathrm{T}}F)^{-1}F^{\mathrm{T}}$ is the Moore–Penrose matrix pseudo-inverse producing the least squares approximation [31]. To initiate the calculation, $\Delta G_{m,1} = G_m - F_m(\vec{u}_0)$ and the first modal weight coefficient is computed as $a_1 = F_m^+(\vec{\varphi}_1)\Delta G_{m,1}$. The process is repeated until the desired set of mass fluxes is satisfied. The solution process is akin to a perturbation expansion where the source function, $\vec{u}_0$ in (3), acts as the leading order solution and each modal contribution serves as the next order correction. The difference from traditional perturbation methods is that the successive corrections occur in state space to satisfy the desired mass fluxes, without considering the remainder of the domain. This is a highly desirable property as the exact velocity profile on the boundary of a complex flow may be unknown. Since POD modes are solutions to the governing equations (to within a multiplicative constant), they contain physically correct velocity profiles and satisfy the divergence free condition. The pressure term in (1b) can be viewed as a Lagrange multiplier to enforce the divergence-free condition of (1a), however the solenoidal condition of $\vec{\varphi}$ eliminates the need to account for the pressure term.

Before the reduced-order methodology can be demonstrated, a prescription for choosing the source function must be described. In a parametric flow, different modes should become more or less important under various parameter values [32]. The source term should then be a function of the mass flux goals, $\vec{u}_0(G_m)$, which can be accomplished by choosing a member of the ensemble as the source function and constructing the POD subspace as an orthogonal complement. This method is superior to the standard mean-centered POD method (referred to as simply the POD from here on), where the source function is taken to be the ensemble mean because solutions 'far' from the mean tend to incur larger errors and this distance from the mean has previously been used as an error measure [20]. Also note, using the mean-centered POD modes in the above flux matching procedure to compute the modal weight coefficients does not guarantee that the boundary conditions for all required approximate solutions within the parameter will be satisfied.

The source function is selected by finding the observation that is geometrically nearest the desired approximation in state space:

$$\min \left\{ \|F_m(\vec{u}^*) - F_m(\vec{u}_k)\|_1 \right\}, \quad k = 1, 2, \ldots, m, \tag{9}$$

with $\vec{u}_0 \subseteq \vec{U}^{\mathrm{obs}}$, the remaining members of the observations form the complement set $\vec{U}'$ which are made orthogonal to the source function. The POD is then performed on $\vec{U}'$ without mean-centering, decomposing the POD subspace into orthogonal complements:

$$\vec{\Phi} = \vec{u}_0 + \vec{\varphi}', \quad \text{where} \quad \vec{u}_0 \in R^{n\times 1} \quad \text{and} \quad \vec{\varphi}' \in R^{n\times m-1}. \tag{10}$$

Thus, the approximation procedure consists of selecting the 'closest' member of the ensemble to the desired solution to serve as the source function and the information about the flow physics contained in the remaining observations is

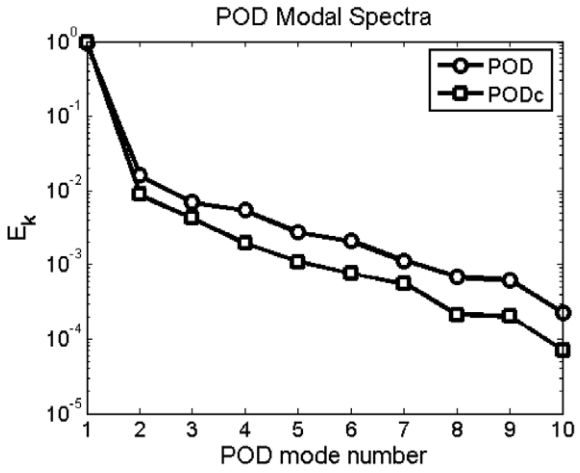

Fig. 3. Mean-centered velocity POD and orthogonal complement POD (PODc) modal energy content.

converted into an orthogonal series expansion about the source function to make higher order corrections to the approximate solution. An important property of this decomposition (referred to as the 'PODc' from here on) is that it does not significantly change the quickly decaying nature of the modal spectrum (see Fig. 3).

To demonstrate this procedure, a test case corresponding to $Re = 36{,}320$ ($\bar{u}^* = 13.33$ m/s in air) was randomly selected, for the configuration shown in Fig. 1. The set of mass flux control surfaces reduces to a single surface coincident with the domain inlet (conversely, the domain outlet could be used to produce the same results by continuity). This simple flow has only a single parameter to be used as a matching condition, indicating the 2-term expansion $\vec{u} = \vec{u}_0 + a_1\vec{\varphi}_1$ is all that is available for the solution approximation. It has been demonstrated that the cumulative energy resolved by the first k modes produces an error bound on the approximation [33]. Fig. 3 shows $E_1 \approx 0.98$, indicating the 2-term approximation should produce errors on the order of 2% in the sense of the L^2-norm. Eq. (11) selects the observation #9 in Table 1, corresponding to $\bar{u} = 13.0$ m/s, as the source function.

Fig. 4(a) illustrates the decaying error in the velocity magnitude for the 1- and 2-term approximate solutions. Fig. 4(b) plots the exact solution and the approximate velocity field in the vicinity of the leading edge of the first block, which is where Fig. 4(a) shows the maximum error occurs. Both Fig. 4(a) and (b) show that approximate

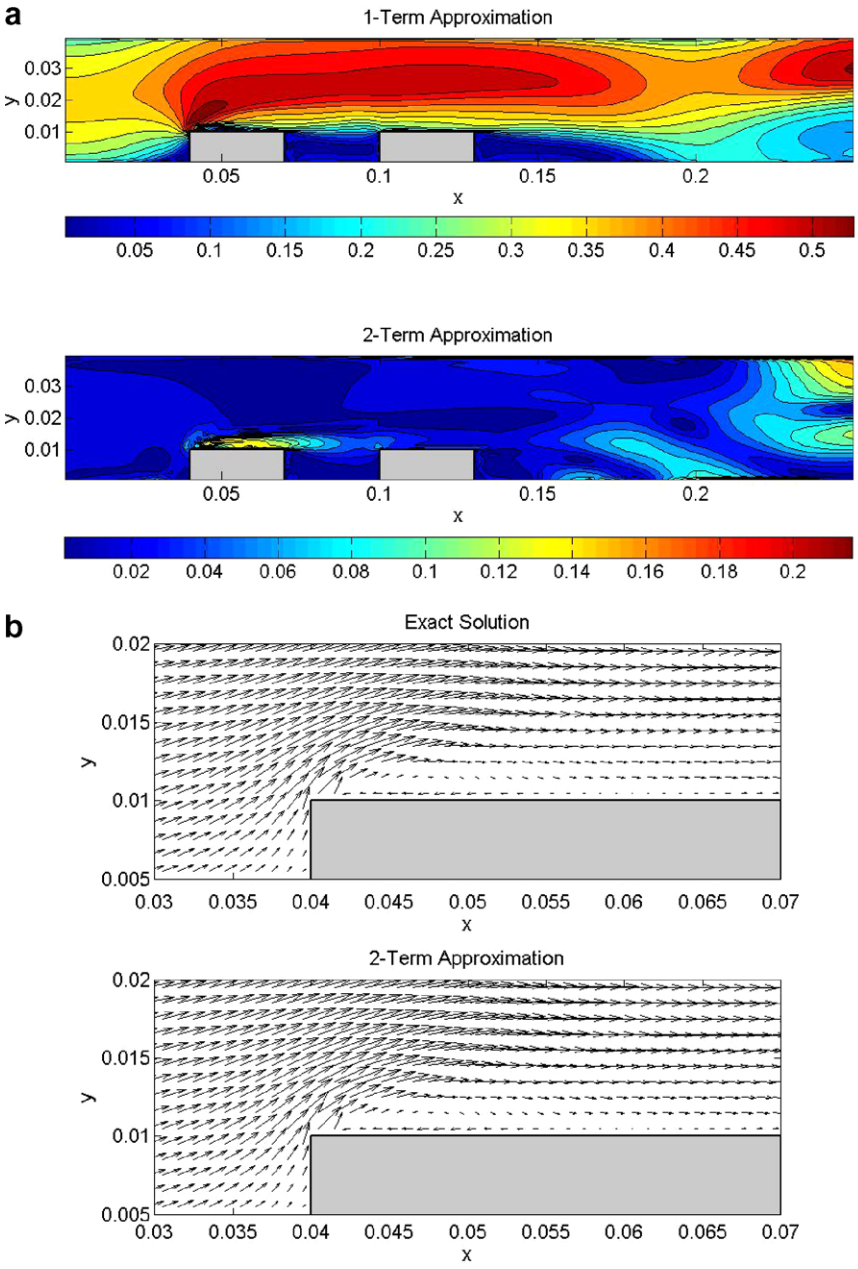

Fig. 4. (a) Velocity absolute approximation error (m/s) and (b) detailed local velocity fields.

solution is very accurate especially considering the full CFD model requires 50,000 DOF and the reduced-order model contains only 2 DOF. The 2-term approximation captures the inlet velocity profile exactly, produces a maximum absolute point-wise error of 0.232 m/s and an L^2 – error norm over the domain of 0.003. Even though the observation space is dense with various mass flow rates, weighted averaging and scaling observations will generally result in poor approximations. For example, rescaling the observation with the difference in mass flow rate from the nearest observation ($\bar{u} = 13.0$ m/s) produces errors three times as large as the PODc based approximation.

At this point, it is reiterated that this reduced-order modeling procedure has been demonstrated on significantly more complex flows, comprised of multiple control surfaces, with very successful results [23] and the objective of the present study is to couple the energy equation into the methodology to extend the low-dimensional modeling framework to convective flows. As the system grows in complexity and more parameters are incorporated, more matching conditions are generated, which requires more modes to be retained in the approximation. Thus, the level of approximation keeps pace with growing system complexity.

7. Low-dimensional turbulent convection modeling

An efficient and accurate reduced-order modeling methodology for turbulent flows has been demonstrated in the previous section, and the objective is now to extend the procedure to include a low-dimensional solution to the energy equation. The orthogonal complement POD and flux matching procedure from the previous section will be employed because of their simplicity, and the main challenge will be in coupling the temperature and velocity fields. To begin, independent velocity and temperature decompositions will be assumed:

$$\vec{u} = \vec{u}_0 + \sum_i a_i \vec{\varphi}_i \quad \text{and} \quad T = T_0 + \sum_j b_j \psi_j. \tag{11}$$

The temperature POD modes are computed with the same procedure, given the temperature observation matrix $\Theta = \{T_1, T_2, \ldots, T_m\} \in R^{n\times m}$.

A natural way to couple the velocity and temperature fields is the Galerkin projection, but as with the RANS momentum equation, the RANS energy equation would require k_{eff} to be specified. Thus, substituting the approximate velocity field $\vec{u}^*$ into (1c) and projecting onto the subspace spanned by $\Psi = \{\psi_1, \psi_2, \ldots, \psi_m\}$ is considered ineffective here.

The flux matching procedure will be extended to include the energy equation, accordingly the heat flux function can be defined analogous to (7) as

$$F_{\text{h}}(T) = \int_{\Gamma_{\text{h}}} -k \frac{\mathrm{d}T}{\mathrm{d}\hat{n}} \mathrm{d}x. \tag{12}$$

The heat flux control surfaces correspond to the 3 surfaces of each block exposed to the airflow. Alternatively, the bottom surface of each block where the heat flux is applied could also be used as the control surface because the system is steady.

POD modes are solutions to the governing Eqs. (1a)–(1c) and inhomogeneous modes can be viewed as a solution with arbitrary boundary conditions. The flux functions (6) and (12) define an inverse problem of finding the corresponding boundary conditions. When the flux function involves a gradient, approximation with discrete data can produce large errors, especially if the gradient is sharp relative to the measurement point spacing. This can be especially difficult if the observations were generated through CFD/HT data, where wall functions were used to alleviate near-wall grid resolution requirements when integrating the turbulence transport equations. Temperature wall functions based on $T^+(y^+) \equiv (T_{\text{w}} - T_{\text{p}})\rho c_p u_t / q''_{\text{w}}$ are used to link the wall boundary condition to the temperature in the first grid cell, T_{p}. When generating the observations either T_{w} or q''_{w} is specified, but in the temperature POD modes, only T_{p} is known, rendering the evaluation of wall heat flux or temperature an under-determined problem.

The wall fluxes can be evaluated by recalling that the method of snapshots expresses the POD modes as a linear combination of the observations. This can generally be written as

$$\vec{\Phi} = L\vec{U}, \tag{13}$$

although the linear transform L cannot be written explicitly because it involves a SVD operation. If the POD procedure is thought of as finding the principle axes of the data contained in $\vec{U}$, then L can be though of as the $m \times m$ rotation matrix between $\vec{U}$ and $\vec{\Phi}$. The transformation matrix L can be computed as the projection of the observations onto the modes utilizing the pseudo-inverse again and the modal fluxes can be directly computed, viz,

$$L = \vec{U}^+ \vec{\Phi} \tag{14a}$$

$$F_m = (v^{\text{T}} L)^{\text{T}}. \tag{14b}$$

The vector v defines the observation mass fluxes and the transpose operation in (14b) is to maintain the same dimension between F_m and v. Defining the temperature observation matrix and the associated matrix of block heat inputs, Q, the modal heat flux can be computed as:

$$F_{\text{h}} = (Q^{\text{T}} T^+ \Psi)^{\text{T}}. \tag{15}$$

This procedure can be used to evaluate any flux function that defines the same quantity contained in the goal vector G regardless of where Γ is located in the domain.

A new method for coupling the temperature field to the velocity field needs to be devised. Ideally, the temperature source function would be a solution to (1c) with $\vec{u}^*$ as the velocity field and corresponding k_{eff}. Then, the linearity of (1c) for a known $\vec{u}$ and k_{eff} could be used to rescale the solution as $T_0 = cT(\vec{u}^*)$. An approximation to this

would be to borrow the temperature field associated with $\vec{u}_0$ and use the POD modal expansion to perturb the solution until the boundary conditions are satisfied. Source function scaling can also be used to improve the approximation since it is treated as the dominant mode of a linear system:

$$T_0 = cT(\vec{u}_o) + \sum_{i=1}^{p} b_i \psi_i. \tag{16}$$

Reasonably accurate temperature field solutions may possibly be obtained without implicitly coupling the velocity field, however this would disregard (1c), possibly producing unphysical results and lack the rigor needed for a robust methodology intended for more complex flows. The implicit coupling and source function scaling introduce no additional complexities implementing (17) algorithmically. The same PODc procedure of (10,11) is employed on the temperature observations with:

$$\Psi = \psi_0 + \psi', \quad \text{where} \quad \psi_0 = T(\vec{u}_0(G_m)) \quad \text{and} \quad \psi' \in R^{n\times m-1}. \tag{17}$$

To scale the source function properly, concatenate $\psi = [\psi_0 \quad \psi']$ and apply the sequential flux matching procedure of (9a–c) as

$$\Delta G_{h,i} = G_{h,i-1} - F_h(T_{i-1}), \tag{18a}$$

$$b_i = F_h^+(\psi_i)\Delta G_{h,i}, \tag{18b}$$

$$T_i = \sum_{j=1}^{i} b_j \psi_j. \tag{18c}$$

8. Results

To demonstrate the reduced-order temperature solution, the previous test case of $Re = 36{,}320$ ($\vec{u}^* = 13.33$ m/s) will be used in the arbitrary $G_h = [Q_1 \quad Q_2] = [96 \quad 66]$W. Fig. 5 plots the POD and PODc temperature modal spectra and it can be seen that the PODc produces a slightly steeper spectrum in the lower order modes. This is a favorable property, as resolving more of the dominant physics with fewer modes allows one to truncate the expansion (16) earlier for a given accuracy requirement. It is generally the case that the temperature spectrum decays less sharply than the velocity spectrum, as noted by other researchers [1], implying more temperature modes are required for the same order of accuracy as the velocity approximation. Fig. 6(a) illustrates a few basic mean-centered POD modes and Fig. 6(b) shows the PODc modes, both for a section of the domain near the heated blocks surface where the largest temperature gradients occur. The PODc procedure produces different temperature modes than the POD procedure because the PODc formulates the modes as a function of parameter values contained in G, converting $\psi(x) \to \psi(x, G_h)$.

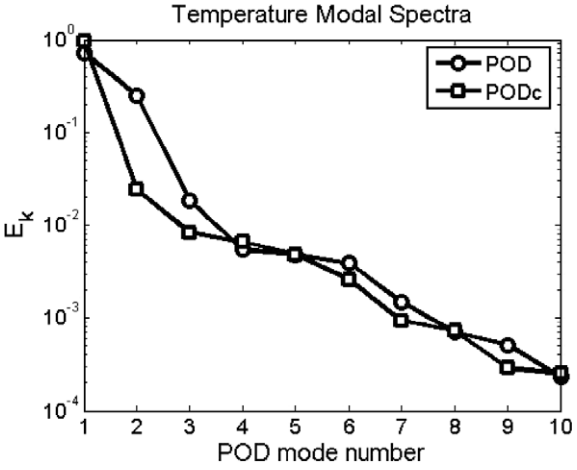

Fig. 5. Temperature modal spectra for the POD and PODc procedures.

Using all $p = 10$ modes, the implicit coupling has a maximum point-wise error of 0.529 °C. The relative error over the domain and boundary condition satisfaction is defined as

$$T_{err,k} = \frac{\|T_k^* - T_{exact}\|_2}{\|T_{exact}\|_2}, \tag{19a}$$

$$Q_{err,k} = \frac{\|F_h(T_k^*) - F_h(T_{exact})\|_2}{\|F_h(T_{exact})\|_2} = \frac{\|F_h(T_k^* - T_{exact})\|_2}{\|F_h(T_{exact})\|_2}, \tag{19b}$$

and the implicit coupling procedure with the PODc subspace and flux matching method of evaluating the weight coefficients produced $T_{err} = 0.0322$ and $Q_{err} = 4.17 \times 10^{-4}$ Fig. 7 illustrates the exact and approximate solutions. The largest errors occur near the surface of the blocks where the largest temperature gradients occur. A large truncation in system DOF can allow the dominant physics to be captured, but at the expense of some small-scale features being discarded, usually in the form of sharp gradients. However, these errors are of the order of 3%, making the temperature approximation quite accurate considering the system was reduced to 10 DOF from the original 60,000 DOF required to compute the turbulent flow and heat transfer. The approximate solution shows a slight overly diffusive temperature field near the trailing edge of both blocks, which may be partially attributed to a finite error between desired and approximate solution boundary conditions.

Both velocity and temperature low-dimensional models are constructed by using a linear subspace to describe the physics for a range of parameters. Poor approximations will result for the nonlinear RANS momentum Eq. (1b) if the POD or PODc procedures are used outside the parameter range, however the linearity of Eq. (1c) with known $\vec{u}^*$ and k_{eff} allows one to predict a temperature field from any parameter value as long as $\vec{\Phi}$ and Ψ subspaces adequately describe the physics. If the boundary heat fluxes were large enough to induce significant buoyancy or even phase change in the case of a liquid medium, the Ψ subspace would not describe the thermal physics, for instance. For an inlet Reynolds number of $Re = 23{,}221$ ($\bar{u} = 8.48$ m/s) and block power dissipation of

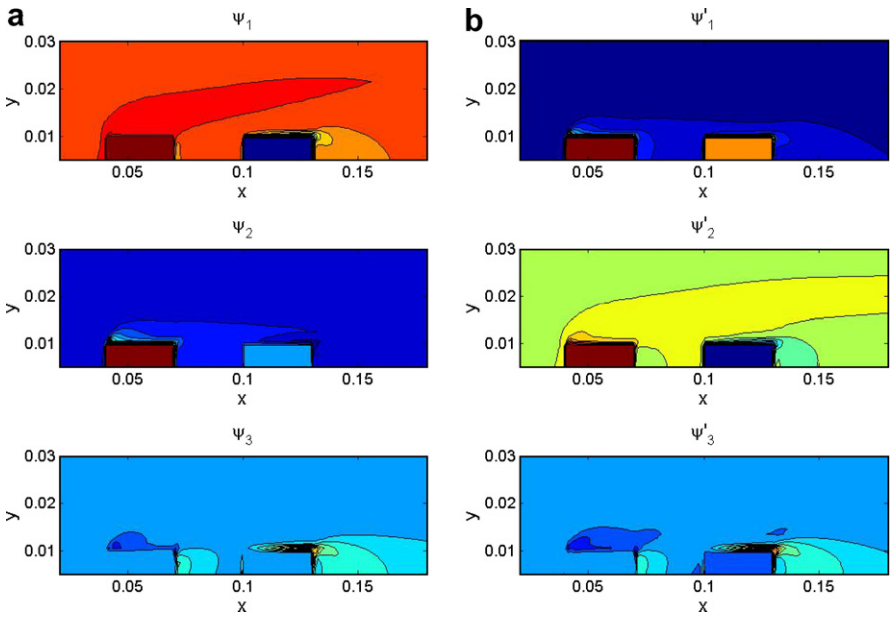

Fig. 6. Local (a) mean-centered POD modes and (b) PODc modes for test case.

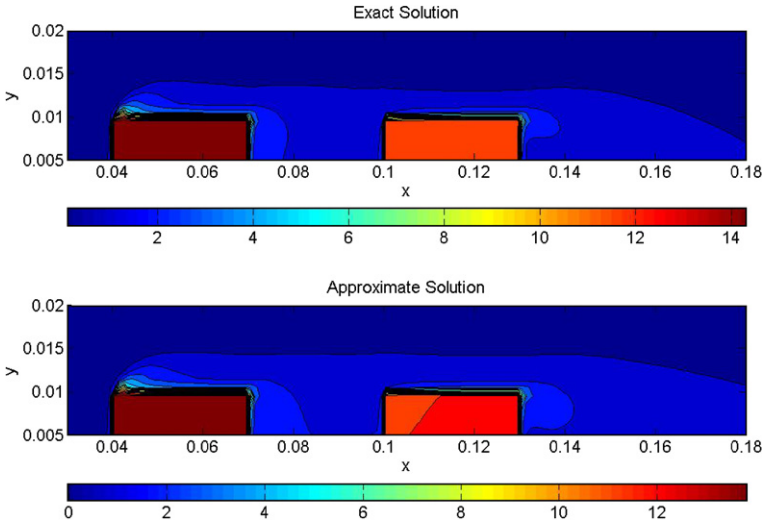

Fig. 7. Exact and approximate temperature fields (°C).

$G_h = [Q_1 \quad Q_2] = [349 \quad 475]$W, the maximum point-wise temperature error was 3.07 °C (out of a maximum of 127 °C) and $T_{err} = 0.0227$. The integral boundary condition formulation was satisfied to $Q_{err} \sim 10^{-5}$. The approximate velocity field had a maximum 0.48 m/s maximum error and a relative L^2-error of 0.0043. Note the observation data in Table 1 ranges from $1/8 \leqslant Q1/Q2 \leqslant 8$, so it is reasonable to expect that any forced convection flow within the parameter range of Re and Q_1/Q_2 would perform with comparable accuracy.

9. Error analysis

In the POD methodology, the question of the minimum number of modes to be retained in the reduced-order model often arises. The Galerkin projection produces m-coupled ODE's in time for the weight coefficient evolution and reducing the number of equations to be integrated in time can result in significant economies for long term dynamics investigations. The objective here was to produce accurate steady models using the minimum number of system observations. In either case, it must be demonstrated that the POD subspaces ($\vec{\Phi}$ and Ψ) sufficiently capture the system physics. Some authors use projection energy of the un-retained POD modes as a total error estimate $\|e\| = 1 - E_{1\to m} = \frac{\sum_{k=p+1}^{m} \lambda_k}{\sum_{k=1}^{m} \lambda_k}$, although this assumes there is no in-plane error [33]. Note $\|\cdot\|$ denotes the 2-norm throughout this section unless otherwise noted. The parametric modeling methodology is based on a low number

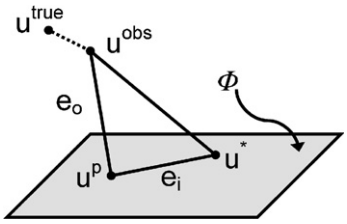

Fig. 8. POD subspace in-plane (e_i) and out-of-plane (e_i) error component schematics.

of system observations, leading to a relatively few number of basis functions and generally requiring that most, if not all, modes will be retained.

Rathnam and Petzold [34] divide the error into the subspace projection error (e_o) and in-plane error associated with evaluating the modal weight coefficients (e_i). Fig. 8 schematically depicts this error partitioning for a general POD subspace Φ, where u^{obs} is the system observation to be approximated, u^* is the approximate POD solution and u^p is the affine orthogonal projection of u^{obs} onto Φ and represents the best POD approximation of u^{obs}. To show Φ contains sufficient information, the a posteriori error estimate of $\|e_o\| \approx 0$ can be used, or at least $\|e_o\| \ll \|e_i\|$, showing the error is dominated by the in-plane contribution. For the approximate temperature solution presented in Section 8, $\|e_o\| = \|T^p\| - \|T^{obs}\| = O(10^{-4})$, consistent with the Q_{err} boundary error, implying the temperature POD modes adequately capture the system physics.

The error between the observation and the 'true' solution will not be considered as it is the user's task to ensure that numerical or experimental data faithfully represent the true system. The POD model (u^*) is an efficient solution to the full model (u^{obs}) and only describes the physics contained within Φ. Thus, the low-dimensional model can never be more accurate that the full model in the sense of being closer to the true solution, but it can produce nearly as accurate results as the full model in an exceedingly more efficient manner.

To examine the convergence of the sequential solution procedure of Eqs. (8(a)–(c)) and (18(a)–(c)), a dual weighted residual technique [35] will be used. Consider the canonical non-square optimization problem:

$$\min\left\{\left\|G - \sum_i a_i F_i\right\|\right\} \rightarrow Fa = G. \tag{20}$$

This could be solved directly in a least squares manner as $a = F^+G$ where $F^+ = (F^TF)^{-1}F^T$ is the pseudo-inverse defined above. The POD modes are normalized and ordered in descending projection energy so the modal weight coefficient magnitude should generally decay. Computing the $a_i's$ sequentially will mimic this spectral decay because the goal residual will decrease with each successive mode while computing the vector of $a_i's$ all at once as F^+G does not guarantee this decrease in magnitude.

Define d as the vector of distances between the approximate weight coefficients (a^*) and the projected weight coefficients ($\tilde{a}$). The true projected and approximate solutions to (20) are then:

$$F\tilde{a} = G(\text{true projected solution}), \tag{21a}$$

$$Fa^* = G(\text{approximate solution}). \tag{21b}$$

The error functional is defined as $J(a) = d^Ta$, resulting in an error of $J(\tilde{a}) - J(a^*) = J(e) = (e,d)$ and a residual of $r = G - Fa^*$. The boundary condition error in state space (e) is analogous to the in-plane error (e_i) in the POD subspace. Note a small residual does not imply a small error. The dual problem can then be formulated as a linear problem driven by the error functional, see (22), and the error functional can be expressed:

$$F^Ta' = d, \tag{22}$$

$$J(e) = (e,d) = (e,Fa') = (F^Te,a') = (r,a'). \tag{23}$$

The fourth term in (23) was derived from the third term using Lagrange's identity $(u,Kv) = (\widehat{K}u,v)$ where $\widehat{K}$ is the adjoint of K, which reduces to K^T for $K \in R$. From (23) it can be deduced that the error for the ith term in the sequential solution is bounded by:

$$|J(e)|_i \leqslant \sum_{k=1}^{i}(|r_k\|a_k'|). \tag{24}$$

This estimate provides a posteriori error bound because knowledge of the vector of perturbations from the true projected solution is required. Fig. 9 plots the temperature error and error bound for the test case presented in Section 8. The decrease in the error bound with increasing modes implies the sequential matching procedure is weakly convergent.

The POD subspace representation of the physics has been demonstrated to be adequate and the sequential flux matching procedure has shown to be bounded and weakly converges to the desired boundary conditions. However, the overall objective is to demonstrate how well the

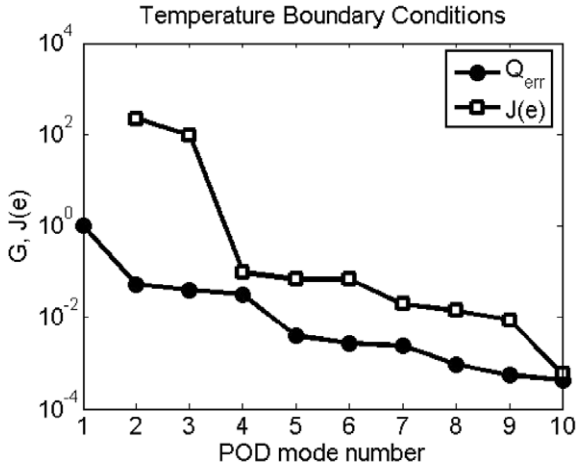

Fig. 9. Temperature flux matching procedure error and error bounds.

reduced-order model approximates the full model. Consider a full nonlinear steady model in the canonical form $N(u) = 0$, $u \in R^n$. The reduced-order canonical solution of the form $u = u_0 + \sum_{i=1}^{m} a_i \varphi_i$ can be expressed in the POD subspace $\Phi = \{\varphi_1, \varphi_2, \ldots, \varphi_m\}$ through the action of the orthogonal projector P from Section 4 as $\tilde{u} = P^{\mathrm{T}}(u - u_0) + u_0$, $P \in R^{n \times m}$. The full (u) and reduced-order approximate (u^*) solutions can be written as [34]

$$u = P^{\mathrm{T}}x + (P')^{\mathrm{T}}z + u_0 = P^{\mathrm{T}}x - e_{\mathrm{o}} + u_0, \tag{25a}$$

$$u^* = P^{\mathrm{T}}x + P^{\mathrm{T}}y + u_0 = P^{\mathrm{T}}x + e_i + u_0, \tag{25b}$$

where P' is the orthogonal complement to P. As above, the approximations will employ all m POD modes such that $\|e_{\mathrm{o}}\| \approx 0$ rendering $u \approx \tilde{u}$. Solving for the in-plane error $e_{\mathrm{i}} = P^{\mathrm{T}}y$ and substituting in the modal expansion gives:

$$\begin{aligned} y &= (P^{\mathrm{T}})^{+}(u^* - u_0 - P^{\mathrm{T}}x) = (P^{\mathrm{T}})^{+}(u^* - \tilde{u}) \\ &= (P^{\mathrm{T}})^{+}\left(\sum_i a_i^* \phi_i - \sum_i \tilde{a}_i \phi_i\right) \\ &= (P^{\mathrm{T}})^{+}\sum_i \phi_i (a^* - \tilde{a})_i. \end{aligned} \tag{26}$$

Returning to the thermal test case, it can be seen that the projection matrix is simply the concatenation of the temperature POD modes, $P = \Psi = \{\psi_1, \psi_2, \ldots, \psi_m\}$ such that $\Psi^{\mathrm{T}} T^{\mathrm{obs}} = b$. Since Ψ is an orthogonal matrix, $\Psi \sum_{i=1}^{m} \psi_i = I \in R^m$, (26) reduces to

$$y = a_i^* - \tilde{a}_i = -d. \tag{27}$$

Comparison of the reduced-order approximation to an affine projection of the full model on the POD subspace produces the same error estimate as the adjoint problem to the boundary condition error. Therefore, the boundary condition error bound is the in-plane error estimate $\|e_{\mathrm{i}}\|$, which suggests the implicit assumption of matching only the relevant control surface integral conditions in the flux matching procedure is valid and leads to unique approximate solutions. As a final note, the triangle inequality can be used to bound the total error $\|e_{\mathrm{o}} + e_{\mathrm{i}}\| \leqslant \|e_{\mathrm{o}}\| + \|e_{\mathrm{i}}\|$ even though $\|e_{\mathrm{o}}\| \ll \|e_{\mathrm{i}}\|$ for parameter values within the predefined range.

10. Conclusions

The traditional POD methodology has been reformulated to treat parametric turbulent forced convective flows for a predefined range of flow boundary conditions. Orthogonal complement POD subspaces were introduced to satisfy inhomogeneous boundary conditions, eliminating the additional effort required by homogenization procedures and extending the reduced-order methodology to a wide range of flows. A flux matching procedure was formulated to evaluate the modal weight coefficients after the standard methods of Galerkin projection and extended state vectors were shown to be ineffective for parametric turbulent forced convection. An implicit coupling procedure was developed to link the temperature and velocity fields, greatly improving the accuracy of low-dimensional temperature predictions. The overall reduced-order modeling framework presented here was able to condense a numerical model requiring 60,000 DOF to 20 DOF for an order 10^3 reduction, while still retaining greater that 95% accuracy over the domain. Rigorous a posteriori error bounds show that the flux matching procedure is an accurate and computationally superior approach for low-dimensional modeling of nonlinear steady turbulent convection.

The methodology presented here is equally applicable to experimental data and could be used to create low-dimensional models of stochastically characterized systems and integrated into large-scale simulations, creating an experimentally validated computationally efficient modeling methodology for complex systems. Slightly less accurate models may be far superior to large expensive models during early system design and optimization, where many different parameter values and component interactions may need to be evaluated. The low-dimensional framework developed here also has the advantage of characterizing distributed parameter systems in state space integral conditions, alleviating the need to specify detailed flow and heat transfer profiles that are often unknown. It also does not require the evaluation of the governing equations, making it well suited for inverse problems and parameter identification studies.

Acknowledgements

The authors acknowledge support for this research from the Office of Naval Research under contract number N00014-04-1-0335, monitored by Dr. Mark Spector.

References

[1] X. Ma, G.E. Karniadakis, H.M. Park, M. Gharib, *DPIV/T*-driven convective heat transfer simulation, Int. J. Heat Mass Transfer 45 (2002) 3517–3527.
[2] B. Shapiro, Creating compact models for electronic systems: An overview and suggested use of existing model reduction and experimental system identification tools, IEEE Trans. Components, Packaging, and Manuf. Technol. A 26 (1) (2003) 165–172.
[3] P. Holmes, J.L. Lumley, G. Berkooz, Turbulence, Coherent Structures, Dynamical Systems and Symmetry, Cambridge University Press, Great Britain, 1996.
[4] A.E. Deane, I.G. Kevrekidis, G.E. Karniadakis, S.A. Orszag, Low-dimensional models for complex geometry flows: Application to grooved channels and circular cylinders, Phys. Fluids A 3 (10) (1991) 2337–2354.
[5] H.M. Park, O.Y. Kim, Reduction of modes for the control of viscous flows, Int. J. Eng. Sci. 39 (2001) 177–200.
[6] S.S. Ravindran, A reduced order approach to optimal control of fluids using proper orthogonal decomposition, Int. J. Numer. Methods Fluids 34 (5) (2000) 457–478.
[7] S.S. Ravindran, Control of flow separation over a forward-facing step by model reduction, Comput. Methods Appl. Mech. Eng. 191 (2002) 1924–1942.
[8] X. Ma, G.E. Karniadakis, A low-dimensional model for simulating three-dimensional cylinder flows, J. Fluid Mech. 458 (2002) 181–190.

[9] H.M. Park, D.H. Cho, The use of the Karhunen–Loeve decomposition for the modeling of distributed parameter systems, Chem. Eng. Sci. 51 (1) (1996) 81–98.
[10] H.M. Park, D.H. Cho, Low dimensional modeling of flow reactors, Int. J. Heat Mass Transfer 39 (16) (1996) 3311–3323.
[11] L. Sirovich, H.M. Park, Turbulent thermal convection in a finite domain: Part I, Theor. Phys. Fluids 2 (9) (1990) 1649–1657.
[12] L. Sirovich, H.M. Park, Turbulent thermal convection in a finite domain: Part II. Numerical results, Phys. Fluids 2 (9) (1990) 1649–1657.
[13] I.H. Tarman, L. Sirovich, Extensions of Karhunen–Loeve based approximations of complicated phenomena, Comput. Methods Appl. Mech. Eng. 155 (1998) 359–368.
[14] H.M. Park, W.J. Li, Boundary optimal control of natural convection by means of mode reduction, J. Dyn. Syst. Meas. Control 124 (2002) 47–54.
[15] S. Sirisup, G.E. Karniadakis, Stability and accuracy of periodic flow solutions obtained by a pod-penalty method, Physica D 202 (2005) 218–237.
[16] J.A. Taylor, M.N. Glauser, Towards practical flow sensing and control via pod and lse based low-dimensional tools, ASME J. Fluids Eng. 126 (2004) 337–345.
[17] Y. Utturkar, B. Zhang, W. Shyy, Reduced-order description of fluid flow with moving boundaries by proper orthogonal decomposition, Int. J. Heat Fluid Flow 26 (2005) 276–288.
[18] B. Galletti, C.H. Bruneau, L. Zannetti, A. Iollo, Low-order modeling of laminar flow regimes past a confined square cylinder, J. Fluid Mech. 503 (2004) 161–170.
[19] H.V. Ly, H.T. Tran, Modeling and control of physical processes using proper orthogonal decomposition, Math. Comput. Model. 33 (2001) 223–236.
[20] E.A. Christensen, M. Brons, J.N. Sorensen, Evaluation of proper orthogonal decomposition—based techniques applied to parameter dependent nonturbulent flows, SIAM J. Sci. Comput. 21 (4) (2000) 1419–1434.
[21] B.H. Jorgensen, J.N. Sorensen, M. Brons, Low-dimensional modeling of a driven cavity flow with two free parameters, Theor. Comput. Fluid Dyn. 16 (2003) 299–317.
[22] D. Rempfer, On low-dimensional galerkin models for fluid flow, Theor. Comput. Fluid Dyn. 14 (2) (2000) 75–88.
[23] J. Rambo, Y. Joshi, Reduced order modeling of steady turbulent flows using the pod, ASME Summer Heat Transfer Conference, San Francisco, CA, 2005.
[24] J. Rambo, Reduced-order modeling of multiscale turbulent convection: Application to data center thermal management, Ph.D. thesis, Georgia Institute of Technology, Atlanta, GA, 2006.
[25] S.-Y. Yoo, J.-H. Park, M.-H. Chung, Local heat transfer characteristics in simulated electronic modules, ASME J. Electron. Packaging 125 (2003) 362–368.
[26] B. Kader, Temperature and concentration profiles in fully turbulent boundary layers, Int. J. Heat Mass Transfer 24 (9) (1981) 1541–1544.
[27] Y.-M. Chen, K.-C. Wang, Experimental study on the forced convection flow in a channel with heated blocks in tandem, Exp. Therm. Fluid Sci. 16 (1998) 286–298.
[28] W.P. Jones, B.E. Launder, The calculation of low-Reynolds-number phenomena with a two-equation model of turbulence, Int. J. Heat Mass Transfer 16 (1973) 1119–1130.
[29] A.K. Saha, S. Acharya, Unsteady simulation of turbulent flow and heat transfer in a channel with periodic array of cubic pin-fins, Numer. Heat Transfer A 46 (8) (2004) 731–763.
[30] L. Sirovich, Turbulence and the dynamics of coherent structures. Parts I–III, Quarterly of Appl. Math. XLV (3) (1987) 561–590.
[31] R. Penrose, A generalized inverse for matrices, Proc. of Cambridge Philos. Soc. 51 (1955) 406–413.
[32] M.D. Graham, I.G. Kevrekidis, Alternative approaches to the Karhunen–Loeve decomposition for model reduction and data compression, Comput. Chem. Eng. 20 (5) (1996) 495–506.
[33] O.K. Rediniotis, J. Ko, A. Kurdilla, Reduced order nonlinear Navier–Stokes models for synthetic jets, J. Fluids Eng. 124 (2002) 433–443.
[34] M. Rathnam, L.R. Petzold, A new look at proper orthogonal decomposition, SIAM J. Numer. Anal. 41 (5) (2003) 1893–1925.
[35] M. Meyer, H.G. Matthies, Efficient model reduction non-linear dynamics using the Karhunen–Loeve expansion and dual-weighted-residual methods, Comput. Mech. 31 (2003) 179–191.